

On Polar Coding with Feedback

Ling Liu¹, Qi Cao¹, Liping Li², Baoming Bai¹

¹Guangzhou Institute of Technology, Xidian University, Guangzhou, China

²Key Laboratory of Intelligent Computing and Signal Processing Ministry of Education, Anhui University, Hefei, China
liuling@xidian.edu.cn, caoqi@xidian.edu.cn, liping_li@ahu.edu.cn, bmbai@mail.xidian.edu.cn

Abstract—In this work, we investigate the performance of polar codes with the assistance of feedback in communication systems. Although it is well known that feedback does not improve the capacity of memoryless channels, we show that the finite length performance of polar codes can be significantly improved as feedback enables genie-aided decoding and allows more flexible thresholds for the polar coding construction. To analyze the performance under the new construction, we then propose an accurate characterization of the distribution of the error event under the genie-aided successive cancellation (SC) decoding. This characterization can be also used to predict the performance of the standard SC decoding of polar codes with rates close to capacity.

I. INTRODUCTION

Feedback has become an increasingly indispensable resource in modern communication systems. For reliable communications, the receiver sends “ACK/NACK” signals back to the transmitter to decide whether a re-transmission round is needed in the TCP/IP protocol. The more efficient hybrid automatic repeat request (HARQ) protocol tries to make use of the received data and some incremental redundancy to recover the message. With the assistance of the so-called 1-bit feedback, rateless codes [1] or fountain codes [2] were proposed for broadcast channels, which provide better rate compatibility than traditional forward error correction codes. For wireless communications, feedback is playing a crucial role as it conveys channel state information, which triggers the beamforming, pre-coding and a series of optimization schedules on the sending side.

In this work, we focus on the design of channel coding in the presence of feedback. Although Shannon proved that using feedback does not improve the capacity of memoryless point-to-point channels, it certainly changes the trade-off between error probability and complexity for erasure correction. A celebrated evidence is the coding scheme proposed by Schalkwijk and Kailath [3], named as the SK coding for additive white Gaussian noise (AWGN) channels. It achieves the capacity with doubly exponential decay in the error probability, which is better than the best random coding without feedback. Note that the SK coding was originally designed using noiseless feedback, and it has been subsequently extended to the noisy feedback and secure communication scenarios [4], [5].

As a kind of capacity achieving codes, polar codes have received widespread attentions since their invention in 2008. In the original work [6], Arıkan proposed the successive cancellation (SC) decoding algorithm, which is sub-optimal

in finite block length yet still sufficient to show the capacity-achieving result. Since then, researchers have made great efforts to improve the performance of polar codes by more sophisticated decoding methods, such as belief propagation decoding, successive cancellation list (SCL) decoding [7] and successive cancellation hybrid (SCH) decoding [8]. Notably, with the assistance of cyclic redundancy check (CRC), polar codes under the CRC aided SCL decoding exhibits high competitiveness compared to LDPC and Turbo codes. More recently, Arıkan proposed the polarization adjusted convolutional (PAC) codes [9], which demonstrated the capability of achieving the dispersion approximation bound. An excellent survey on the development of polar codes can be found in [10]. It appears that existing techniques for polar codes are close to reaching the performance limit in the absence of feedback, perhaps it is time to introduce feedback to probe for further improvement potential. To the best of our knowledge, there is a limited body of literature on polar codes with feedback. In [11], the authors proposed a scheme using a feedback link to return the potentially erroneous positions for short polar codes. A repetition code is then required to indicate the value of the querying bit. The optimized strategy for this scheme is still unknown.

The rest of the paper is organized as follows: Sect. II gives preliminaries of polar codes and a brief review of the SK coding. The feedback polar coding scheme is described in Sect. III, where we also provide a detailed performance analysis of our coding scheme. In Sect. IV, we show the simulation results and how this analysis can be utilized for other related problems. The paper is concluded in Sect. V.

Notation : All random variables (RVs) are denoted by capital letters. Let $P(X)$ denote the probability mass function of a RV X taking values in a countable set \mathcal{X} . The combination of N i.i.d. copies of X is denoted by a vector X_1^N or $X^{[N]}$, where $[N] = \{1, \dots, N\}$, and its i -th element is given by X_i . The subvector of $X^{[N]}$ with indices limited to a subset $\mathcal{F} \subseteq [N]$ is denoted by $X^{\mathcal{F}}$. The cardinality of \mathcal{F} is $|\mathcal{F}|$. The expectation and variance of a RV are denoted by $E[\cdot]$ and $\text{Var}[\cdot]$, respectively. We use binary logarithm \log throughout this paper.

II. PRELIMINARIES OF POLAR CODES AND THE SK CODING SCHEME

A. Polar Codes for Channel Coding

Denote by W a binary-input memoryless symmetric channel (BMSC) with uniform input $X \in \mathcal{X}$ and output $Y \in \mathcal{Y}$. Its

channel transition probability is given by $P_{Y|X}$. The Shannon capacity of W is denoted by $C(W)$. Let $N = 2^n$ for some positive integer n . The polarization matrix is defined as

$$\mathbf{G}_N \triangleq \begin{bmatrix} 1 & 0 \\ 1 & 1 \end{bmatrix}^{\otimes n} \times \mathbf{B}_N, \quad (1)$$

where \otimes denotes the Kronecker product, and \mathbf{B}_N is the bit-reverse permutation matrix [6]. The matrix \mathbf{G}_N transforms N identical copies of W into a vector channel $W_N : U^{[N]} \rightarrow Y^{[N]}$, where $U^{[N]} = X^{[N]}\mathbf{G}_N^{-1}$ is the polarized version of the input $X^{[N]}$. Notice that $\mathbf{G}_N^{-1} = \mathbf{G}_N$ in \mathbb{F}_2 . W_N can be successively split into N binary memoryless symmetric synthetic channels $U^i \rightarrow (U_1^{i-1}, Y^{[N]})$, denoted by $W_N^{(i)}$ with $1 \leq i \leq N$. The core of channel polarization states that, as N increases, $W_N^{(i)}$ polarizes to a good (roughly error-free) channel or a totally noisy one almost surely. Moreover, the fractions of these two extreme synthetic channels turn to $C(W)$ and $1 - C(W)$, respectively. To achieve the capacity, one can choose a rate $R = \frac{K}{N}$ smaller than $C(W)$, transmit information bits through K good synthetic channels, and feed frozen bits (commonly set to all-zero) to the rest ones.

The indices of good or bad synthetic channels can be identified based on their associated Bhattacharyya parameters.

Definition 1. Given a BMSC W with transition probability $P_{Y|X}$, the Bhattacharyya parameter of W is defined as

$$Z(W) \triangleq \sum_y \sqrt{P_{Y|X}(y|0)P_{Y|X}(y|1)}. \quad (2)$$

For performance analysis, the Bhattacharyya parameter provides an upper-bound on the average error probability $P_e(U^i|U_1^{i-1}, Y^{[N]})$ in estimating U^i on the basis of U_1^{i-1} and $Y^{[N]}$ via the maximum a posteriori probability (MAP) decision rule. In [12], the rate of polarization β is analyzed to characterize how fast $Z(W_N^{(i)})$ approaches 0 or 1. For the 2-by-2 kernel $\begin{bmatrix} 1 & 0 \\ 1 & 1 \end{bmatrix}$, β is upper-bounded by $\frac{1}{2}$. That is, for any $0 < \beta < \frac{1}{2}$, we have

$$\lim_{N \rightarrow \infty} P(Z(W_N^{(i)}) < 2^{-N^\beta}) = C(W), \quad (3)$$

and

$$\lim_{N \rightarrow \infty} P(Z(W_N^{(i)}) > 1 - 2^{-N^\beta}) = 1 - C(W). \quad (4)$$

As a result, when the information set is chosen as $\mathcal{I} = \{i \in [N] : Z(W_N^{(i)}) < 2^{-N^\beta}\}$ for channel coding, the block error probability under the SC decoding can be bounded as

$$P_e^{SC} \leq N \cdot 2^{-N^\beta}. \quad (5)$$

B. The SK Feedback Coding

The SK feedback coding scheme was firstly proposed for the scalar AWGN channel with a noiseless and power-unconstrained feedback link. For initialization, the interval $[-\sqrt{3}, \sqrt{3}]$ is divided into $M = 2^{NR}$ isometric subintervals, the middle points of which correspond to the M messages for transmission. Let θ denote the RV chosen from the set of points with probability $1/M$. One can check that $E[\theta] = 0$ and

$E[\theta^2] = 1$ when M is sufficiently large. For the 1st round, the transmitter sends symbol $X_1 = \sqrt{P}\theta$, where P is the power constraint. Then, $Y_1 = X_1 + Z_1$ is received, where Z_1 is the Gaussian noise RV with zero mean and unit variance. Y_1 is then perfectly feedbacked to the transmitter. For the 2nd round, the transmitter calculates $\epsilon_1 = \frac{Y_1 - X_1}{\sqrt{P}}$ and sends $X_2 = \frac{\sqrt{P}}{\sqrt{\text{Var}[\epsilon_1]}}\epsilon_1$. After receiving $Y_2 = X_2 + Z_2$, the receiver performs MMSE estimation for ϵ_1 and obtains $\hat{\epsilon}_1$, which is then feedbacked for the next round. For the i -th round, where $i \geq 3$, let $\epsilon_{i-1} = \epsilon_{i-2} - \hat{\epsilon}_{i-2}$ and $X_i = \frac{\sqrt{P}}{\sqrt{\text{Var}[\epsilon_{i-1}]}}\epsilon_{i-1}$. Based on $Y_i = X_i + Z_i$, the MMSE estimate $\hat{\epsilon}_{i-1}$ of ϵ_{i-1} is obtained and then feedbacked. This process repeats iteratively until $i = N$. For the recovery of θ , notice that $\theta = \frac{X_1}{\sqrt{P}}$, which can be expanded as

$$\begin{aligned} \frac{X_1}{\sqrt{P}} &= \frac{Y_1}{\sqrt{P}} - \epsilon_1 \\ &= \frac{Y_1}{\sqrt{P}} - \hat{\epsilon}_1 - (\epsilon_1 - \hat{\epsilon}_1) \\ &= \underbrace{\frac{Y_1}{\sqrt{P}} - \sum_{i=1}^{N-1} \hat{\epsilon}_i}_{\hat{\theta}} - \epsilon_N, \end{aligned} \quad (6)$$

where $\hat{\theta}$ is treated as the estimate of θ as Y_1 and all $\hat{\epsilon}_i$'s are available at the receiver. An error event occurs when ϵ_N is larger than half of the subinterval size. By the property of MMSE, $\frac{\text{Var}[\epsilon_i - \hat{\epsilon}_i]}{\text{Var}[\epsilon_i]} = \frac{1}{P+1}$ for each step, which yields $\text{Var}[\epsilon_N] = \frac{1}{P} \left(\frac{1}{P+1}\right)^{N-1}$. Therefore, the error probability of the SK coding can be upper-bounded as

$$P_e^{SK} \leq 2Q\left(\frac{\sqrt{3}/2^{NR}}{\sqrt{\text{Var}[\epsilon_N]}}\right) = 2Q(\delta \cdot 2^{N(C-R)}), \quad (7)$$

where $Q(\cdot)$ denotes the Q-function, δ is a constant depends on P , and C is the capacity of the AWGN channel. A geometric interpretation of the first three rounds in the SK coding scheme is shown in Fig. 1, where the squared Euclidean distance represents the variance of a RV.

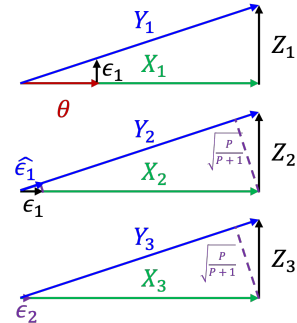


Fig. 1. A geometric interpretation of the SK coding scheme.

III. POLAR FEEDBACK CODING

A. The Coding Scheme

The SK code provides a concrete example of how to use feedback to design a capacity-achieving code with good performance. However, the scalar form makes it incompatible with existing communication systems. We are more concerned with applying its underlying principles to improve the performance of existing block codes, particularly polar codes, which have been integrated into both 5G and future 6G standards.

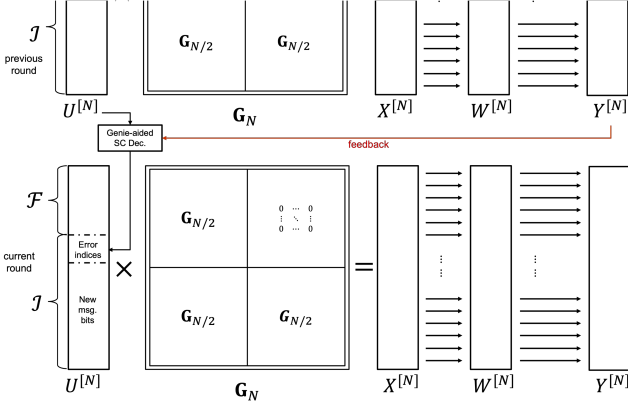


Fig. 2. Block diagram of the polar feedback coding scheme.

Our proposed polar feedback coding scheme is depicted in Fig. 2, where a series of polar coding blocks is chained by a feedback link. Suppose that a communication round has already been completed using standard polar coding. That is, the information bits and frozen bits are stitched into $U^{[N]}$, which is encoded to $X^{[N]}$ by G_N . The $X^{[N]}$ is then fed into N i.i.d. copies of a BMSC W , producing output $Y^{[N]}$. Next, we assume that $Y^{[N]}$ is feedbacked to the transmitter before the following transmission round. Following the principle of the SK coding, one may perform a proper estimation of $U^{[N]}$ based on $Y^{[N]}$, and send the estimation error back to the receiver. Since $U^{[N]}$ is available at the transmitter, it turns out the estimate can be obtained efficiently by a genie-aided (GA)-SC decoding algorithm. The estimation error is then represented by the following set of error-bit indices:

$$\mathcal{T} \triangleq \{i \in \mathcal{I} : \hat{U}_i \neq U_i\}, \quad (8)$$

where \hat{U}_i is the hard decision of the SC decoder based on $Y^{[N]}$ and its preceding bits U_1^{i-1} . We note that since the GA-SC decoder eliminates the error propagation effect of the standard SC decoder, the size $|\mathcal{T}|$ is significantly smaller than the case when $U^{[N]}$ is not available, as shown in [13]. Each index in \mathcal{T} can be described by a $\log N$ -bit sequence and the estimation error requires $|\mathcal{T}| \times \log N$ bits. Unlike the SK coding, the next transmission is not solely dedicated to convey the estimation error. Instead, we append $K - |\mathcal{T}| \times \log N$ new information bits to maintain the dimension of polar codes, which is more convenient for practical implementation. By doing so, we have assembled $U^{[N]}$ for the next coding block. At the receiver, standard SC decoding is utilized to

test whether $U^{[N]}$ can be recovered from $Y^{[N]}$ at each round with the aid of CRC. The rate loss caused by the CRC is ignored for simplicity. Once it succeeds, the previous coding blocks can be decoded in a reversed order when \mathcal{T} is available. The delay D ($D \geq 1$) of decoding is defined such that the j -th block is successfully decoded by the time the $(j + D - 1)$ -th block is received. This process proceeds iteratively until all information bits has been successively decoded. We temporarily assume that the buffer is of adequate size at the receiver side, meaning that the maximum delay tolerance $D_{\max} = \infty$.

Remark 1. Using a polar decoding algorithm for error estimation indeed endows the feedback link with a certain degree of noise tolerance. In practice, $Y^{[N]}$ can be converted into log-likelihood ratio with a certain level of quantization precision. As long as the decoding algorithm is synchronized between the two sides, a noisy version of $Y^{[N]}$ is also acceptable for our scheme. For convenience of description, however, we simply assume that $Y^{[N]}$ is perfected returned.

Theorem 1. For the proposed ideal feedback model, the optimal construction of polar codes in terms of coding rate is given by:

$$\mathcal{F} \triangleq \left\{ i \in [N] : P_e(U_i|U_1^{i-1}, Y^{[N]}) > \frac{1}{\log N} \right\}, \quad (9)$$

and $\mathcal{I} = \mathcal{F}^c$, where $\frac{1}{\log N}$ is called the optimal threshold ϵ_{th}^* .

Proof: If $P_e(U_i|U_1^{i-1}, Y^{[N]}) > \frac{1}{\log N}$, putting i in the frozen set \mathcal{F} costs 1-bit rate loss. However, putting i in \mathcal{I} costs average rate loss

$$P_e(U_i|U_1^{i-1}, Y^{[N]}) \cdot \log N > 1 \quad (10)$$

for the next round. For the first round, no error index exists, which can be viewed as a closed-loop coding scheme that always starts with $\mathcal{T} = \emptyset$. From a long-term perspective, the influence of the initial state on the coding rate is negligible. ■

Remark 2. Compared with the construction of polar codes without feedback in Section II, where the threshold is chosen as 2^{-N^β} , we see that feedback helps to relax the threshold to $\frac{1}{\log N}$, which results in a higher coding rate for finite block length.

As a validation of Theorem 1, we present the Monte Carlo simulation results for our coding scheme with different thresholds ϵ_{th} in Table I, where W is a binary symmetric channel (BSC) with crossover probability 0.11. It can also be observed that the average delay varies dramatically with ϵ_{th} . Under the optimal threshold ϵ_{th}^* , the average delay exceeds 10; moreover, the simulated maximum delay can be over 100, which is impractical for real-world applications. In the next section, we investigate the relationship between D and ϵ_{th} and show that the performance of our scheme can be precisely predicted.

TABLE I
PERFORMANCE OF POLAR CODES WITH $N = 2^{10}$ AND DIFFERENT THRESHOLDS OVER BSC(0.11).

Threshold ϵ_{th}	$\frac{1}{3}\epsilon_{\text{th}}^*$	$\frac{1}{2}\epsilon_{\text{th}}^*$	$\frac{1}{1.5}\epsilon_{\text{th}}^*$	ϵ_{th}^*	$\frac{1}{0.8}\epsilon_{\text{th}}^*$	$\frac{1}{0.5}\epsilon_{\text{th}}^*$
Average rate	0.407	0.416	0.422	0.426	0.424	0.407
Average delay \bar{D}	2.168	3.102	4.879	10.340	22.847	131.933

B. Performance Analysis

It is clear that the delay D follows a geometric distribution with successive probability $P(\hat{U}^{\mathcal{I}} = U^{\mathcal{I}})$ and \bar{D} is equal to its reciprocal. Evaluating $P(\hat{U}^{\mathcal{I}} = U^{\mathcal{I}})$ is equivalent to evaluating P_e^{SC} . The union bound $\sum_{i \in \mathcal{I}} P_e(U_i | U_1^{i-1}, Y^{[N]})$ mentioned in Section II generally provides a tight upper bound on P_e^{SC} when ϵ_{th} is close to 0. However, when $\epsilon_{\text{th}} = O(\frac{1}{\log N})$, this union bound could be useless as it can exceed 1. To better predict the performance of this scheme, we turn to investigate the distribution of the size $|\mathcal{T}|$, which can be characterized by only a few parameters.

Given that $|\mathcal{T}| = \sum_{i \in \mathcal{I}} \mathbb{1}(\hat{U}_i \neq U_i)$, our first observation is that $E[|\mathcal{T}|]$ can be obtained as follows.

$$E[|\mathcal{T}|] = \sum_{i \in \mathcal{I}} E[\mathbb{1}(\hat{U}_i \neq U_i)] = \sum_{i \in \mathcal{I}} P_e(U_i | U_1^{i-1}, Y^{[N]}), \quad (11)$$

where $P_e(U_i | U_1^{i-1}, Y^{[N]})$ can be estimated within acceptable precision using the methods in [14].

Remark 3. It is noted that $P(\hat{U}^{\mathcal{I}} \neq U^{\mathcal{I}}) = P(|\mathcal{T}| \neq 0)$. Using the Markov inequality, we have

$$P(|\mathcal{T}| \geq 1) \leq \frac{E[|\mathcal{T}|]}{1} = \sum_{i \in \mathcal{I}} P_e(U_i | U_1^{i-1}, Y^{[N]}), \quad (12)$$

which is a restatement of the union bound for P_e^{SC} , and it may explain why this is not tight when $E[|\mathcal{T}|]$ is not near 0.

We then investigate the variance $\text{Var}[|\mathcal{T}|]$ of $|\mathcal{T}|$. To do so, the second moment $E[|\mathcal{T}|^2]$ is expressed as

$$\begin{aligned} E[|\mathcal{T}|^2] &= E \left[\sum_{i \in \mathcal{I}} \mathbb{1}(\hat{U}_i \neq U_i) \sum_{j \in \mathcal{I}} \mathbb{1}(\hat{U}_j \neq U_j) \right] \\ &= E \left[\sum_{i \in \mathcal{I}} \mathbb{1}(\hat{U}_i \neq U_i) \sum_{j=i} \mathbb{1}(\hat{U}_j \neq U_j) \right] \\ &\quad + E \left[\sum_{i \in \mathcal{I}} \mathbb{1}(\hat{U}_i \neq U_i) \sum_{j \neq i, j \in \mathcal{R}(i)} \mathbb{1}(\hat{U}_j \neq U_j) \right] \\ &\quad + E \left[\sum_{i \in \mathcal{I}} \mathbb{1}(\hat{U}_i \neq U_i) \sum_{j \neq i, j \in \mathcal{R}^c(i)} \mathbb{1}(\hat{U}_j \neq U_j) \right], \end{aligned} \quad (13)$$

where $\mathcal{R}(i)$ is defined as the error indices that are correlated with the index i . The first term on the r.h.s. of the above equality is $E[|\mathcal{T}|]$. For the third term, based on the results in [15] and [16], we claim that the majority of the error indices tend to be uncorrelated with each other. Moreover, when ϵ_{th}

is chosen as $O(\frac{1}{\log N})$, the product of two expectations of two error events is less than $O(\frac{1}{\log^2 N})$, which is insignificant compared to $E[|\mathcal{T}|]$. Therefore, the third term can be approximated by $E^2[|\mathcal{T}|]$. Rearranging the equation yields the following approximation for the second term.

$$\begin{aligned} \text{Var}[|\mathcal{T}|] - E[|\mathcal{T}|] &\approx E \left[\sum_{i \in \mathcal{I}} \mathbb{1}(\hat{U}_i \neq U_i) \sum_{j \neq i, j \in \mathcal{R}(i)} \mathbb{1}(\hat{U}_j \neq U_j) \right]. \end{aligned} \quad (14)$$

Characterizing the exact pattern of $\mathcal{R}(i)$ is nontrivial. Alternatively, we adopt an ‘‘amortized’’ approach to view the occurrence of error event. The key idea is to uniformly distribute error events across r_{fit} disjoint subsets of information indices, with the assumption that correlations are confined within each subset. That is, the second term is decoupled by letting $\sum_{j \neq i, j \in \mathcal{R}(i)} \mathbb{1}(\hat{U}_j \neq U_j) = \frac{E[|\mathcal{T}|]}{r_{\text{fit}}}$ for some positive r_{fit} . Since all $E[|\mathcal{T}|]$ errors are assigned to some indices in $\mathcal{R}(i)$ for different i , the index i corresponding to $\mathbb{1}(\hat{U}_i \neq U_i)$ can be viewed as a switching error index and the indices in $\mathcal{R}(i)$ are triggered by such i . Noting that $E[\sum_{i \in \mathcal{I}} \mathbb{1}(\hat{U}_i \neq U_i)]$ equals $E[|\mathcal{T}|]$, there are r_{fit} such switching indices. The error occurrence in $\mathcal{R}(i)$ is then modeled as a geometric process (starts with index 0) with successive probability p_{fit} , which captures the possibility that the next error is a switching error or a triggered error. A toy example with $r_{\text{fit}} = 4$ and $E[|\mathcal{T}|] = 6$ is demonstrated in Fig. 3, with switching error indices indicated by red dashed arrows and triggered error indices by green solid ones. The index of the geometric process is also shown for each of the r_{fit} trials. Note that r_{fit} and $E[|\mathcal{T}|]$ are not necessarily integers; they can also be positive real numbers.

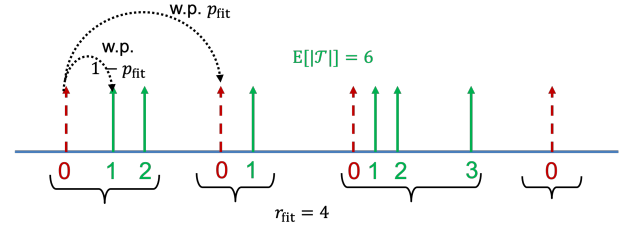


Fig. 3. A statistic perspective of the occurrence of error events.

The above analysis suggests that it is possible to view the RV $|\mathcal{T}|$ as the result of r_{fit} consecutive geometric process with successive probability p_{fit} , which is indeed a *negative binomial* process with number of successes r_{fit} .

Theorem 2. Given $E[|\mathcal{T}|]$ and $\text{Var}[|\mathcal{T}|]$, suppose that X is a RV that follows the negative binomial distribution with $r_{\text{fit}} = \frac{E^2[|\mathcal{T}|]}{\text{Var}[|\mathcal{T}|] - E[|\mathcal{T}|]}$ and $p_{\text{fit}} = \frac{E[|\mathcal{T}|]}{\text{Var}[|\mathcal{T}|]}$, i.e., for $x = 0, 1, 2, \dots$,

$$P_{\text{NB}}(X = x | r_{\text{fit}}, p_{\text{fit}}) = \binom{r_{\text{fit}} + x - 1}{x} p_{\text{fit}}^{r_{\text{fit}}} (1 - p_{\text{fit}})^x, \quad (15)$$

where the binomial coefficient can be expressed equivalently using Euler’s Gamma function for real r_{fit} . Then, $E[X] = E[|\mathcal{T}|]$ and $\text{Var}[X] = \text{Var}[|\mathcal{T}|]$.

Proof: Note that the negative binomial process is made up by r_{fit} identical geometric processes. The expectation and variance of the geometric distributions (starts with index 0) with successive probability p_{fit} are $\frac{1-p_{\text{fit}}}{p_{\text{fit}}}$ and $\frac{1-p_{\text{fit}}}{p_{\text{fit}}^2}$, respectively. ■

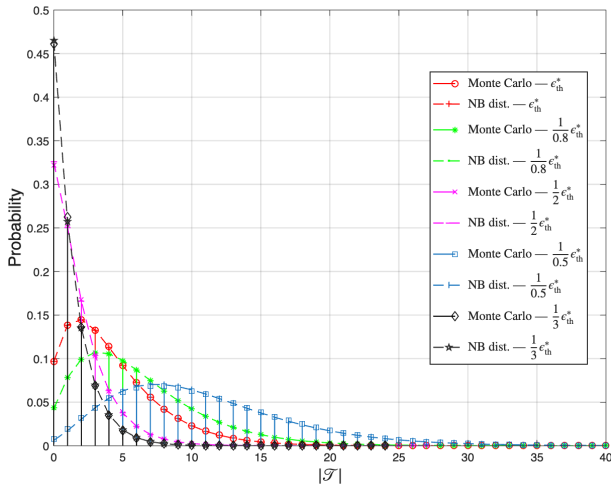


Fig. 4. The fitness of the negative binomial distribution for $|\mathcal{T}|$.

The fitness of the negative binomial distribution for $|\mathcal{T}|$ with varying ϵ_{th} for the same environment as in Table I is illustrated in Fig. 4. Similar results can be obtained when the channel is replaced with a binary erasure channel (BEC) or a binary input AWGN (BIAWGN) channel with BPSK modulation. We see that Theorem 2 provides a good prediction of the distribution of $|\mathcal{T}|$. Consequently, for a specific ϵ_{th} , once $E[|\mathcal{T}|]$ and $\text{Var}[|\mathcal{T}|]$ are known, the successive decoding probability for each round in our feedback coding scheme can be approximated by $P(|\mathcal{T}| = 0) = p_{\text{fit}}^{r_{\text{fit}}}$. Then, the delay D follows a geometric distribution with successive probability $p_{\text{fit}}^{r_{\text{fit}}}$ and $\bar{D} = p_{\text{fit}}^{-r_{\text{fit}}}$. For a finite maximum delay tolerance D_{max} , the decoding failure probability can be also predicted by the sum of the tails of the geometric distribution, which is $(1 - p_{\text{fit}}^{r_{\text{fit}}})^{D_{\text{max}}}$. Recall that $E[|\mathcal{T}|]$ can be obtained from (11). Next, we will show that $\text{Var}[|\mathcal{T}|]$ may also be accurately estimated by investigating the second order statistical properties of the channel polarization process.

Let W be a $\text{BEC}(p)$ with erasure probability p . Consider the polarization process of W with $N = 2^n$. To save the space, we derive the next theorem based on the result of [16]. Before that, we define the erasure event for index i as $\mathcal{E}_i \triangleq \mathbb{1}(\hat{U}_i = ?)$. Since $W_N^{(i)}$ is a BEC for all $i \in [N]$, $E[\mathcal{E}_i] = Z(W_N^{(i)})$. Denote by \mathbf{C}_N the N -by- N covariance matrix of the random vector consist of \mathcal{E}_i for $i \in [N]$, i.e.,

$$\mathbf{C}_N(i, j) \triangleq \text{Cov}[\mathcal{E}_i, \mathcal{E}_j], \quad (16)$$

where $\text{Cov}[X, Y] \triangleq E[XY] - E[X]E[Y]$.

Theorem 3. Consider the polar feedback coding when W is a $\text{BEC}(p)$. The Bhattacharyya parameter $Z(W_N^{(i)})$ can be calculated by applying the transform $(p, p) \rightarrow (2p - p^2, p^2)$ recursively. \mathbf{C}_N can be also calculated based on $\mathbf{C}_{N/2}$ as in

(19) with initial condition $\mathbf{C}_1 = p(1 - p)$. Given a threshold ϵ_{th} for $P_e(U_i|U_1^{i-1}, Y^N)$ and construct \mathcal{I} as in Theorem 1, then,

$$E[|\mathcal{T}|] = \sum_{i \in \mathcal{I}} P_e(U_i|U_1^{i-1}, Y^N) = \frac{1}{2} \sum_{i \in \mathcal{I}} Z(W_N^{(i)}), \quad (17)$$

and

$$\text{Var}[|\mathcal{T}|] = \frac{1}{2} E[|\mathcal{T}|] + \frac{1}{4} \sum_{i \in \mathcal{I}} \sum_{j \in \mathcal{I}} \mathbf{C}_N(i, j). \quad (18)$$

Proof: The first part is straightforward as $P_e(W) = \frac{1}{2} Z(W)$ for BEC. For the second part, (19) is from [16]. The proof is completed by expanding $\text{Var}[|\mathcal{T}|]$ as (20), where the third equality holds because $E[\mathbb{1}(\hat{U}_i \neq U_i)] = \frac{1}{2} E[\mathbb{1}(\hat{U}_i = ?)]$ and $E[\mathbb{1}(\hat{U}_i \neq U_i) \mathbb{1}(\hat{U}_j \neq U_j)] = \frac{1}{4} E[\mathbb{1}(\hat{U}_i = ?) \mathbb{1}(\hat{U}_j = ?)]$ for $i \neq j$ and uniform $U^{\mathcal{I}}$. ■

Fig. 5 demonstrates the validity of Theorem 3 over $\text{BEC}(0.5)$ with varying N and $\epsilon_{\text{th}}^* = \frac{1}{\log N}$. We also plot the results for $\text{BSC}(0.11)$ and BIAWGN channel with standard deviation $\sigma = 0.97865$. An approximately linear relationship between $\frac{\text{Var}[|\mathcal{T}|]}{E[|\mathcal{T}|]}$ and $\log N$ can be observed, at least for N from 2^9 to 2^{14} , which means it is possible to estimate $\text{Var}[|\mathcal{T}|]$ based on $E[|\mathcal{T}|]$ for channels other than BEC. We may also use the BEC approximation [17] or the channel merging methods [14], [18] to evaluate $\text{Var}[|\mathcal{T}|]$ directly for future work.

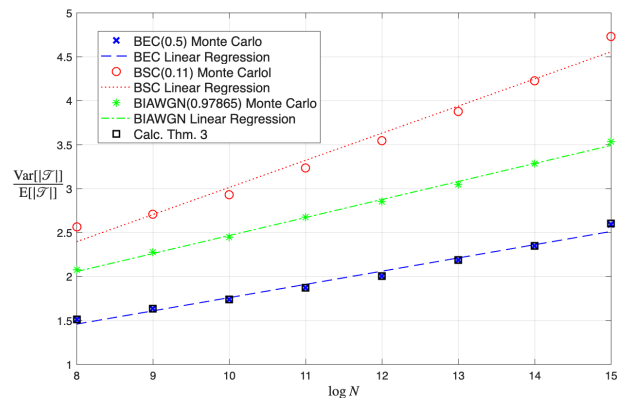


Fig. 5. $\frac{\text{Var}[|\mathcal{T}|]}{E[|\mathcal{T}|]}$ for different BMSCs and N .

IV. SIMULATION RESULTS

The block error rate (BLER) performance of our proposed feedback coding scheme for $\text{BSC}(0.11)$ is shown in Fig. 6. For comparison, the performance curves without feedback are also provided to demonstrate the improvement. When $D_{\text{max}} = \infty$, the system attains theoretical error-free performance. This point is marked at a BLER of 10^{-6} in the figure. For other points, we adjust the threshold ϵ_{th} as in Table I to control the distribution of $|\mathcal{T}|$ and D for different tolerance D_{max} . These points characterize the trade-off between rate and feedback delay. Thanks to Theorem 2, $P(|\mathcal{T}|)$ can be accurately estimated, which, in turn, enables precise prediction of the BLER.

As a by-product, the approximation for $P(|\mathcal{T}| = 0)$ according to Theorem 2 provides a means to predict the

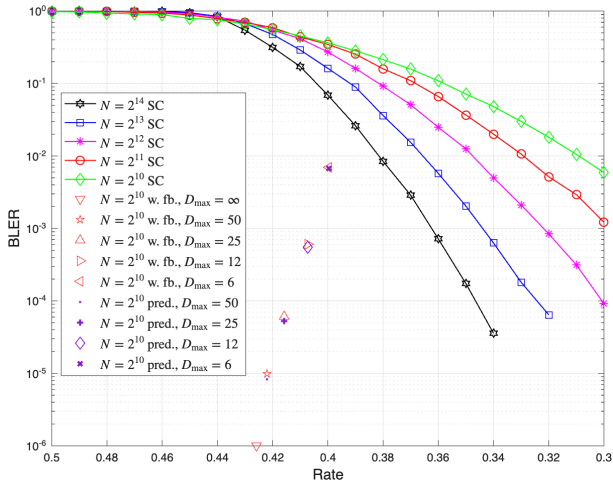


Fig. 6. The error performance of polar feedback coding for BSC(0.11).

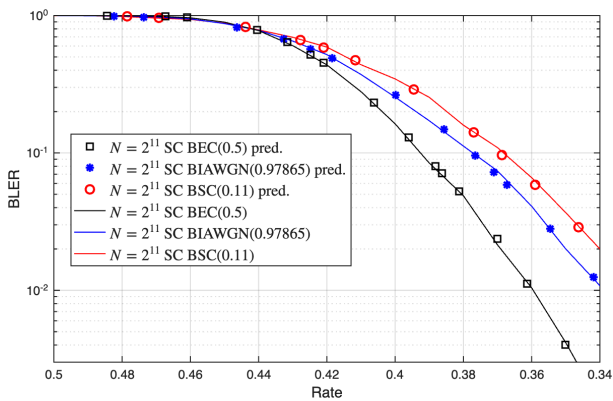


Fig. 7. Predicting the BLER of the standard SC decoding using Theorem 2.

BLER of the standard SC decoder (without feedback). Note that the rate is now $\frac{|\mathcal{T}|}{N}$ instead of $\frac{|\mathcal{T}| - nE[|\mathcal{T}|]}{N}$. In Fig. 7, the block length is set to $N = 2^{11}$ for three typical BMSCs: BEC(0.5), BSC(0.11) and BIAWGN(0.97865). By adjusting the threshold as $\epsilon_{\text{th}} = \frac{1}{\alpha} \epsilon_{\text{th}}^*$ for α from 0.5 to 200, we see that the performance of SC decoding can be well predicted by Theorem 2 using $E[|\mathcal{T}|]$ and $\text{Var}[|\mathcal{T}|]$, which may be computable during the construction of polar codes. Combining our method with the existing tight bounds [12], [14], [16] for lower BLER region, the entire performance curves can be predicted.

As another by-product, we show that Theorem 2 can be employed to compress the number $|\mathcal{T}|$, when the polar lossless coding scheme [19] is operating in a serial data-stream mode, where $|\mathcal{T}|$ is required for truncation. For the i.i.d. Bernoulli (BER) source with probability 0.11 and length $N = 2^{10}$, we derive an empirical estimate of $P(|\mathcal{T}|)$ via Monte Carlo simulation for different thresholds. The entropy of $P(|\mathcal{T}|)$ is denoted by $H(|\mathcal{T}|)$. We then use $P_{\text{NB}}(|\mathcal{T}|)$ from Theorem 2, with entropy $H_{\text{NB}}(|\mathcal{T}|)$, to generate a Huffman dictionary for $|\mathcal{T}|$ and compute its average length \bar{L} . $H(|\mathcal{T}|)$, $H_{\text{NB}}(|\mathcal{T}|)$ and \bar{L} (all in bits) are listed in Table II, which shows the validity of our statistical model.

TABLE II
THE COMPRESSION OF $|\mathcal{T}|$ FOR BER(0.11) AND $N = 2^{10}$, USING THE DISTRIBUTION IN THEOREM 2.

ϵ_{th}	$\frac{1}{3} \epsilon_{\text{th}}^*$	$\frac{1}{2} \epsilon_{\text{th}}^*$	$\frac{1}{1.5} \epsilon_{\text{th}}^*$	ϵ_{th}^*	$\frac{1}{0.8} \epsilon_{\text{th}}^*$	$\frac{1}{0.5} \epsilon_{\text{th}}^*$
$H(\mathcal{T})$	2.0978	2.5739	3.0224	3.5746	3.9960	4.5965
$H_{\text{NB}}(\mathcal{T})$	2.0983	2.5751	3.0240	3.5748	3.9928	4.5844
\bar{L}	2.1026	2.6248	3.0611	3.6002	4.0369	4.6164

V. CONCLUSION

In this work, we investigate the performance of polar codes with feedback. Specifically, we develop a statistical method to characterize the number of error events under the GA-SC decoder, which captures the interplay among coding rate, system delay, and error performance. As a direction for future work, this statistical method can be extended to characterize systems with a limited error index budget—specifically, to analyze the GA- T_{max} SC decoder where T_{max} is the maximum allowable genie corrections. The coding rate can be further improved by compressing \mathcal{T} using our recent work [20]. We also believe that the framework developed here can be applied to advance the finite-length performance analysis [21], [22] of polar codes.

REFERENCES

- [1] A. Shokrollahi, "Raptor codes," *IEEE Trans. Inf. Theory*, vol. 52, no. 6, pp. 2551–2567, 2006.
- [2] D. J. C. Mackay, "Fountain codes," *IEE Proc. Part I, Commun.*, vol. 152, no. 6, pp. 1062–1068, 2005.
- [3] J. Schalkwijk and T. Kailath, "A coding scheme for additive noise channels with feedback-i: No bandwidth constraint," *IEEE Trans. Inf. Theory*, vol. 12, no. 2, pp. 172–182, 1966.
- [4] A. Ben-Yishai and O. Shayevitz, "Interactive schemes for the awgn channel with noisy feedback," *IEEE Trans. Inf. Theory*, vol. 63, no. 4, pp. 2409–2427, 2017.
- [5] B. Dai, C. Li, Y. Liang, Z. Ma, and S. Shamai Shitz, "Impact of action-dependent state and channel feedback on gaussian wiretap channels," *IEEE Trans. Inf. Theory*, vol. 66, no. 6, pp. 3435–3455, 2020.
- [6] E. Arkan, "Channel polarization: A method for constructing capacity-achieving codes for symmetric binary-input memoryless channels," *IEEE Trans. Inf. Theory*, vol. 55, no. 7, pp. 3051–3073, July 2009.
- [7] I. Tal and A. Vardy, "List decoding of polar codes," *IEEE Trans. Inf. Theory*, vol. 61, no. 5, pp. 2213–2226, May 2015.
- [8] K. Chen, K. Niu, and J. Lin, "Improved successive cancellation decoding of polar codes," *IEEE Trans. Commun.*, vol. 61, no. 8, pp. 3100–3107, Aug. 2013.
- [9] E. Arkan, "From sequential decoding to channel polarization and back again," *CoRR*, vol. abs/1908.09594, 2019. [Online]. Available: <http://arxiv.org/abs/1908.09594>
- [10] K. Niu, P. Zhang, J. Dai, Z. Si, and C. Dong, "A golden decade of polar codes: From basic principle to 5g applications," *China Communications*, vol. 20, no. 2, pp. 94–121, 2023.
- [11] K. Vakilinia, D. Divsalar, and R. D. Wesel, "RCA analysis of the polar codes and the use of feedback to aid polarization at short blocklengths," in *Proc. 2015 IEEE Int. Symp. Inf. Theory*, June 2015, pp. 1292–1296.
- [12] E. Arkan and I. Telatar, "On the rate of channel polarization," in *Proc. 2009 IEEE Int. Symp. Inform. Theory*, Seoul, South Korea, June 2009, pp. 1493–1495.
- [13] O. Afisiadis, A. Balatsoukas-Stimming, and A. Burg, "A low-complexity improved successive cancellation decoder for polar codes," in *Proc. IEEE 48th Asilomar Conf. Signals, Syst. Comput.*, Nov 2014, pp. 2116–2120.
- [14] I. Tal and A. Vardy, "How to construct polar codes," *IEEE Trans. Inf. Theory*, vol. 59, no. 10, pp. 6562–6582, Oct. 2013.
- [15] M. Alsan, "Erasures in channel polarization," *IEEE Trans. Inf. Theory*, vol. 71, no. 6, pp. 4125–4136, June 2025.

$$\mathbf{C}_N(i, j) = \begin{cases} 2 \left(1 - Z\left(W_{N/2}^{(\frac{i+1}{2})}\right)\right) \left(1 - Z\left(W_{N/2}^{(\frac{j+1}{2})}\right)\right) \mathbf{C}_{N/2}(\frac{i+1}{2}, \frac{j+1}{2}) + \mathbf{C}_{N/2}(\frac{i+1}{2}, \frac{j+1}{2})^2, & \text{if } i \text{ is odd and } j \text{ is odd} \\ 2 \left(1 - Z\left(W_{N/2}^{(\frac{i+1}{2})}\right)\right) Z\left(W_{N/2}^{(\frac{j+1}{2})}\right) \mathbf{C}_{N/2}(\frac{i+1}{2}, \frac{j}{2}) - \mathbf{C}_{N/2}(\frac{i+1}{2}, \frac{j}{2})^2, & \text{if } i \text{ is odd and } j \text{ is even} \\ 2Z\left(W_{N/2}^{(\frac{i}{2})}\right) \left(1 - Z\left(W_{N/2}^{(\frac{j+1}{2})}\right)\right) \mathbf{C}_{N/2}(\frac{i}{2}, \frac{j+1}{2}) - \mathbf{C}_{N/2}(\frac{i}{2}, \frac{j+1}{2})^2, & \text{if } i \text{ is even and } j \text{ is odd} \\ 2Z\left(W_{N/2}^{(\frac{i}{2})}\right) Z\left(W_{N/2}^{(\frac{j}{2})}\right) \mathbf{C}_{N/2}(\frac{i}{2}, \frac{j}{2}) - \mathbf{C}_{N/2}(\frac{i}{2}, \frac{j}{2})^2, & \text{if } i \text{ is even and } j \text{ is even} \end{cases} \quad (19)$$

$$\begin{aligned} \text{Var}[|\mathcal{T}|] &= \mathbb{E} \left[\sum_{i \in \mathcal{I}} \mathbb{1}(\hat{U}_i \neq U_i) \sum_{j \in \mathcal{I}} \mathbb{1}(\hat{U}_j \neq U_j) \right] - \mathbb{E} \left[\sum_{i \in \mathcal{I}} \mathbb{1}(\hat{U}_i \neq U_i) \right] \mathbb{E} \left[\sum_{j \in \mathcal{I}} \mathbb{1}(\hat{U}_j \neq U_j) \right] \\ &= \frac{1}{2} \mathbb{E} \left[\sum_{i \in \mathcal{I}} \mathbb{1}(\hat{U}_i \neq U_i) \sum_{j=i} \mathbb{1}(\hat{U}_j \neq U_j) \right] + \frac{1}{2} \mathbb{E} \left[\sum_{i \in \mathcal{I}} \mathbb{1}(\hat{U}_i \neq U_i) \sum_{j \neq i} \mathbb{1}(\hat{U}_j \neq U_j) \right] \\ &\quad + \mathbb{E} \left[\sum_{i \in \mathcal{I}} \mathbb{1}(\hat{U}_i \neq U_i) \sum_{j \neq i} \mathbb{1}(\hat{U}_j \neq U_j) \right] - \mathbb{E} \left[\sum_{i \in \mathcal{I}} \mathbb{1}(\hat{U}_i \neq U_i) \right] \mathbb{E} \left[\sum_{j \in \mathcal{I}} \mathbb{1}(\hat{U}_j \neq U_j) \right] \\ &= \frac{1}{2} \mathbb{E}[|\mathcal{T}|] + \frac{1}{4} \mathbb{E} \left[\sum_{i \in \mathcal{I}} \mathbb{1}(\hat{U}_i = ?) \sum_{j=i} \mathbb{1}(\hat{U}_j = ?) \right] + \frac{1}{4} \mathbb{E} \left[\sum_{i \in \mathcal{I}} \mathbb{1}(\hat{U}_i = ?) \sum_{j \neq i} \mathbb{1}(\hat{U}_j = ?) \right] \\ &\quad - \frac{1}{4} \mathbb{E} \left[\sum_{i \in \mathcal{I}} \mathbb{1}(\hat{U}_i = ?) \right] \mathbb{E} \left[\sum_{j \in \mathcal{I}} \mathbb{1}(\hat{U}_j = ?) \right] \\ &= \frac{1}{2} \mathbb{E}[|\mathcal{T}|] + \frac{1}{4} \mathbb{E} \left[\sum_{i \in \mathcal{I}} \mathcal{E}_i \sum_{j \in \mathcal{I}} \mathcal{E}_j \right] - \frac{1}{4} \mathbb{E} \left[\sum_{i \in \mathcal{I}} \mathcal{E}_i \right] \mathbb{E} \left[\sum_{j \in \mathcal{I}} \mathcal{E}_j \right] \\ &= \frac{1}{2} \mathbb{E}[|\mathcal{T}|] + \frac{1}{4} \sum_{i \in \mathcal{I}} \sum_{j \in \mathcal{I}} \mathbf{C}_N(i, j). \end{aligned} \quad (20)$$

- [16] M. Bastani Parizi and E. Telatar, "On the correlation between polarized becs," in *Proc. 2013 IEEE Int. Symp. Inform. Theory*, July 2013, pp. 784–788.
- [17] E. Arıkan, "A performance comparison of polar codes and Reed-Muller codes," *IEEE Commun. Lett.*, vol. 12, no. 6, pp. 447–449, June 2008.
- [18] R. Pedarsani, S. Hassani, I. Tal, and I. Telatar, "On the construction of polar codes," in *Proc. 2011 IEEE Int. Symp. Inform. Theory*, St. Petersburg, Russia, July 2011, pp. 11–15.
- [19] H. S. Cronie and S. B. Korada, "Lossless source coding with polar codes," in *Proc. 2010 IEEE Int. Symp. Inform. Theory*, Austin, TX, June 2010, pp. 904–908.
- [20] L. Liu, J. Wang, C. Chen, L. Ding, Z. Zhu, and B. Bai, "Improved lossless compression based on polar codes," in *Proc. 2025 IEEE Inf. Theory Workshop*, Spet. 2025, pp. 1–6.
- [21] S. H. Hassani, K. Alishahi, and R. L. Urbanke, "Finite-length scaling for polar codes," *IEEE Trans. Inf. Theory*, vol. 60, no. 10, pp. 5875–5898, 2014.
- [22] M. Mondelli, S. H. Hassani, and R. L. Urbanke, "Unified scaling of polar codes: Error exponent, scaling exponent, moderate deviations, and error floors," *IEEE Trans. Inf. Theory*, Dec. 2016.